

Supplemental material for

Carbonaceous aerosol composition in air masses influenced by large-scale biomass burning: a case-study in Northwestern Vietnam

Dac-Loc Nguyen^{1,2,8}, Hendryk Czech^{1,2}, Simone M. Pieber³, Jürgen Schnelle-Kreis¹, Martin Steinbacher³, Jürgen Orasche¹, Stephan Henne³, Olga B. Popovicheva⁴, Gülcin Abbaszade¹, Günter Engling^{5,a}, Nicolas Bukowiecki⁶, Nhat-Anh Nguyen⁷, Xuan-Anh Nguyen⁸, Ralf Zimmermann^{1,2}

¹Joint Mass Spectrometry Centre (JMSC), Cooperation Group “Comprehensive Molecular Analytics” (CMA), Helmholtz Zentrum München, München, 81379, Germany

²Joint Mass Spectrometry Centre (JMSC), Chair of Analytical Chemistry, University of Rostock, Rostock, 18059, Germany

³Empa, Laboratory for Air Pollution/Environmental Technology, Dübendorf, Switzerland

⁴Skobeltsyn Institute of Nuclear Physics, Moscow State University, Moscow, 119991, Russian Federation

⁵Department of Biomedical Engineering and Environmental Sciences, National Tsing Hua University, Hsinchu 30013, Taiwan

⁶Department of Environmental Sciences, University of Basel, Basel, 4056, Switzerland

⁷Hydro-Meteorological Observation Center, Vietnam Meteorological and Hydrological Administration, Ministry of Natural Resources and Environment, Ha Noi, Vietnam

⁸Institute of Geophysics, Vietnam Academy of Science and Technology (VAST), Ha Noi, Vietnam

^anow at: Mobile Source Laboratory Division, California Air Resource Board, El Monte, CA 91731, United States

Correspondence to: Hendryk Czech (hendryk.czech@uni-rostock.de; hendryk.czech@helmholtz-muenchen.de)

Table S1. EC fractions, OC fractions and speciated organic compounds in PM_{2.5} samples, including minimum (min.) and maximum (max.), as well as median, mean, 1st and 3rd quartiles (Q1 and Q3).

	Abbreviation	Unit	Min.	Q1	Median	Q3	Max.	Mean
Organic Carbon fraction	OC1	µg m ⁻³	0.00	0.00	0.12	0.42	1.05	0.23
Organic Carbon fraction	OC2	µg m ⁻³	0.38	0.64	1.21	1.87	7.07	1.73
Organic Carbon fraction	OC3	µg m ⁻³	1.21	2.38	4.11	6.94	15.30	5.23
Organic Carbon fraction	OC4	µg m ⁻³	0.21	0.74	1.58	3.05	7.96	2.25
Pyrolyzed Organic Carbon	OP	µg m ⁻³	0.00	0.03	0.76	2.89	8.29	1.85
Corrected Element Carbon	EC1-OP	µg m ⁻³	0.07	0.62	1.34	3.60	15.31	2.99
Elemental Carbon fraction	EC2	µg m ⁻³	0.06	0.48	1.22	2.05	3.09	1.25
Elemental Carbon fraction	EC3	µg m ⁻³	0.00	0.00	0.04	0.12	0.43	0.10
Organic Carbon	OC	µg m ⁻³	1.82	3.73	6.57	16.0	38.33	11.1
Elemental Carbon	EC	µg m ⁻³	0.13	0.83	2.05	2.98	9.80	2.41
Eicosanoic acid	A-C20	ng m ⁻³	0.03	0.04	0.08	0.23	0.66	0.17
Docosanoic acid	A-C21	ng m ⁻³	0.06	0.15	0.43	1.53	5.85	1.14
Tetracosanoic acid	A-C24	ng m ⁻³	0.05	0.23	0.76	3.00	12.46	2.25
Pentacosanoic acid	A-C25	ng m ⁻³	0.01	0.03	0.16	0.69	3.17	0.53
Hexacosanoic acid	A-C26	ng m ⁻³	0.03	0.12	0.62	2.30	11.38	1.86
Heptacosanoic acid	A-C27	ng m ⁻³	0.00	0.01	0.10	0.44	2.25	0.36
Octacosanoic acid	A-C28	ng m ⁻³	0.00	0.06	0.46	1.87	9.43	1.55
Nonacosanoic acid	A-C29	ng m ⁻³	0.00	0.02	0.04	0.37	1.85	0.30
Triaccontanoic acid	A-C30	ng m ⁻³	0.00	0.02	0.26	1.34	6.58	1.10
Hentriaccontanoic Acid	A-C31	ng m ⁻³	0.00	0.00	0.03	0.12	0.92	0.14
Dotriaccontanoic Acid	A-C32	ng m ⁻³	0.00	0.00	0.13	0.67	3.16	0.52
Galactosan	GAL	ng m ⁻³	0.05	0.14	0.59	1.85	8.98	1.56
Mannosan	MAN	ng m ⁻³	0.68	1.45	5.28	18.6	60.2	12.9
Levoglucosan	LEV	ng m ⁻³	23.4	110	188	580	1710	437
Vanillin	VAH	ng m ⁻³	0.17	0.46	0.94	3.15	11.8	2.31
p-Hydroxybenzoic acid	p-H-acid	ng m ⁻³	0.31	2.12	7.60	43.0	192	34.1
m-hydroxybenzoic acid	m-H-acid	ng m ⁻³	0.35	1.48	4.66	16.6	45.3	10.5
Syringaldehyde	SYAH	ng m ⁻³	0.00	0.63	1.11	6.24	40.2	6.09
Syringic acid	SYA	ng m ⁻³	0.12	0.32	1.37	7.41	47.9	7.73
Vanillic acid	VA	ng m ⁻³	0.14	0.35	2.08	9.58	49.1	9.07
4-Nitrophenol	4-NP	ng m ⁻³	0.40	0.79	2.21	5.23	59.8	6.66
4-Nitrocatechol	4-NC	ng m ⁻³	0.20	0.45	2.32	5.19	616	41.5
2,6-Dimethoxy-4-nitrophenol	2,6-D-4-NP	ng m ⁻³	0.00	0.00	0.59	0.77	6.06	0.81

Eicosane	C20	ng m ⁻³	0.19	0.29	0.52	1.11	2.08	0.78
Heneicosane	C21	ng m ⁻³	0.60	0.85	1.57	2.93	4.69	1.94
Docosane	C22	ng m ⁻³	0.44	0.82	1.85	4.38	11.8	3.12
Tricosane	C23	ng m ⁻³	0.48	1.17	2.70	9.51	17.5	5.31
Tetracosane	C24	ng m ⁻³	0.78	2.05	4.02	7.39	16.1	5.84
Pentacosane	C25	ng m ⁻³	0.45	1.13	3.01	6.14	19.5	4.82
Hexacosane	C26	ng m ⁻³	0.54	1.40	2.29	4.64	16.9	4.02
Heptacosane	C27	ng m ⁻³	0.61	1.68	3.06	10.24	31.0	7.01
Octacosane	C28	ng m ⁻³	0.36	1.03	1.95	4.93	17.8	4.06
Nonacosane	C29	ng m ⁻³	0.53	1.49	4.55	18.46	58.8	12.7
Triaccontane	C30	ng m ⁻³	0.54	0.92	1.73	4.21	11.5	3.10
Hentriaccontane	C31	ng m ⁻³	0.49	1.09	4.59	16.69	43.4	10.4
Dotriaccontane	C32	ng m ⁻³	0.17	0.36	0.82	1.89	6.27	1.48
Tritriaccontane	C33	ng m ⁻³	0.22	0.44	1.63	4.95	14.4	3.47
<hr/>								
Phenanthrene	PHE	ng m ⁻³	0.00	0.09	0.13	0.17	0.33	0.14
Fluoranthene	FLU	ng m ⁻³	0.01	0.03	0.03	0.05	0.09	0.04
Pyrene	PYR	ng m ⁻³	0.01	0.02	0.03	0.05	0.13	0.04
Benz[a]anthracene	BaA	ng m ⁻³	0.01	0.01	0.02	0.04	0.18	0.04
Chrysene	CHR	ng m ⁻³	0.02	0.03	0.03	0.06	0.17	0.05
ΣBenzo[b,k]fluoranthene	BbkF	ng m ⁻³	0.04	0.10	0.16	0.28	0.67	0.23
Benz[e]pyrene	BeP	ng m ⁻³	0.03	0.09	0.16	0.25	0.42	0.19
Benz[a]pyrene	BaP	ng m ⁻³	0.00	0.01	0.02	0.03	0.13	0.03
Perylene	PER	ng m ⁻³	0.00	0.00	0.00	0.02	0.07	0.01
Indeno[1,2,3-cd]pyrene	IcdP	ng m ⁻³	0.02	0.02	0.04	0.05	0.09	0.04
Benzo[ghi]perylene	BghiP	ng m ⁻³	0.00	0.05	0.08	0.16	0.26	0.10
9H-Fluoren-9-one	9HFLUone	ng m ⁻³	0.29	0.48	0.59	0.76	2.24	0.75
1,8-Naphthalic anhydride	NAP-AN	ng m ⁻³	0.12	0.18	0.27	0.95	4.71	0.92
Naphthoic acid	NAP-AC	ng m ⁻³	0.12	0.32	0.77	1.21	9.13	1.62
9,10-Anthracenedione	9,10-AN	ng m ⁻³	0.29	0.48	0.59	0.76	2.24	0.75

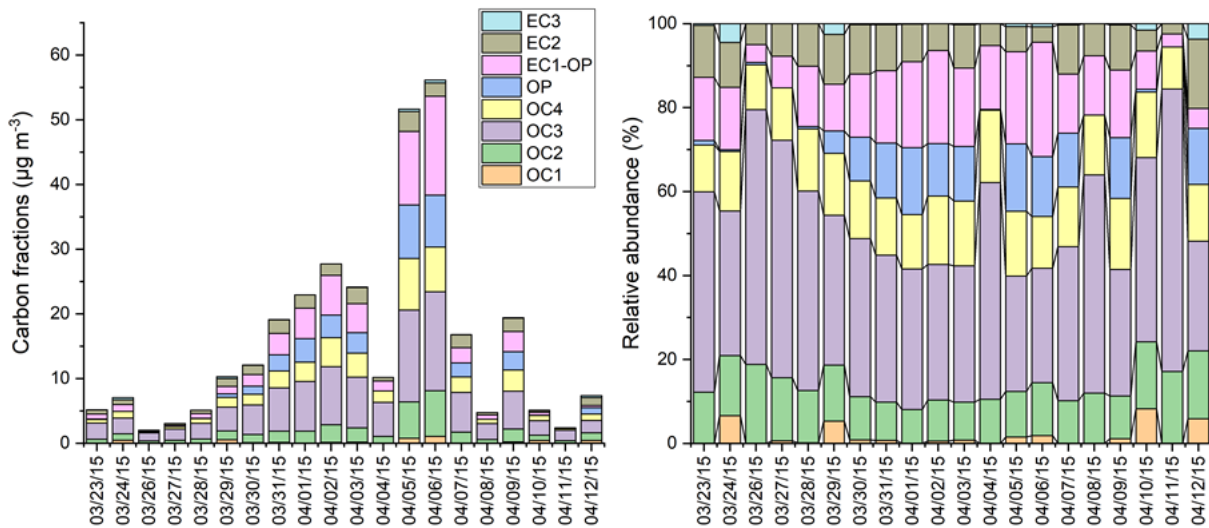


Figure S1. Time series of carbon fractions OC1, OC2, OC3, OC4, OP, EC1-OP, EC2 and EC3 in daily aerosol particle samples ($n=20$) at PDI during the sampling campaign from 23rd March to 12th April 2015. Left column provides concentrations of each carbon fraction ($\mu\text{g m}^{-3}$), and right column provides relative mass fractions within carbonaceous fractions.

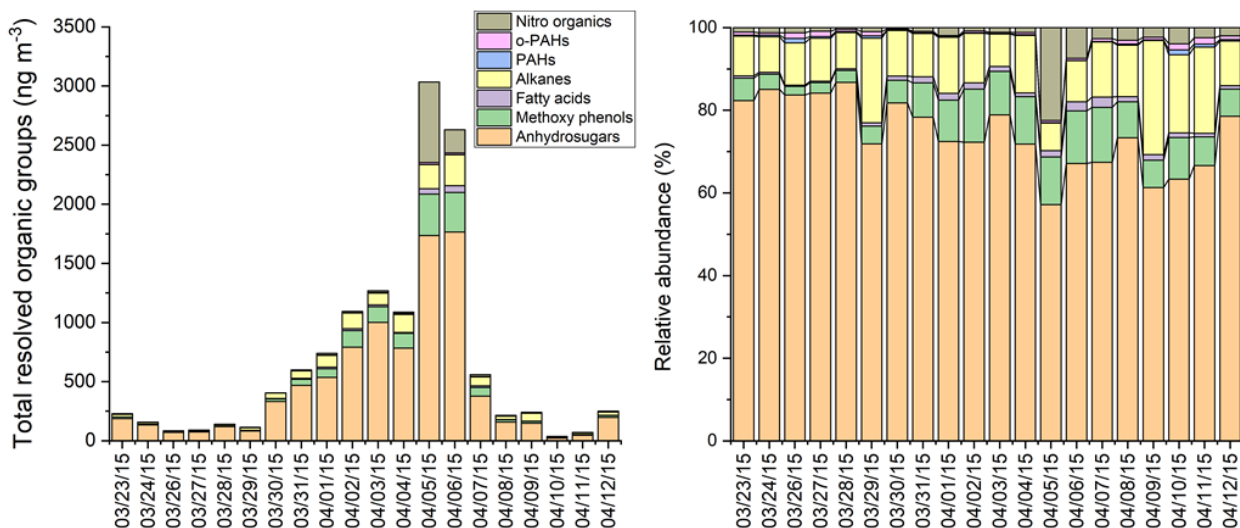


Figure S2. Time series of total resolved organic constituents in daily aerosol particle samples ($n=20$) at PDI during the sampling campaign from 23rd March to 12th April 2015. Left column provides identified mass concentrations ($\mu\text{g m}^{-3}$), and right column provides relative mass fractions within total class of compounds

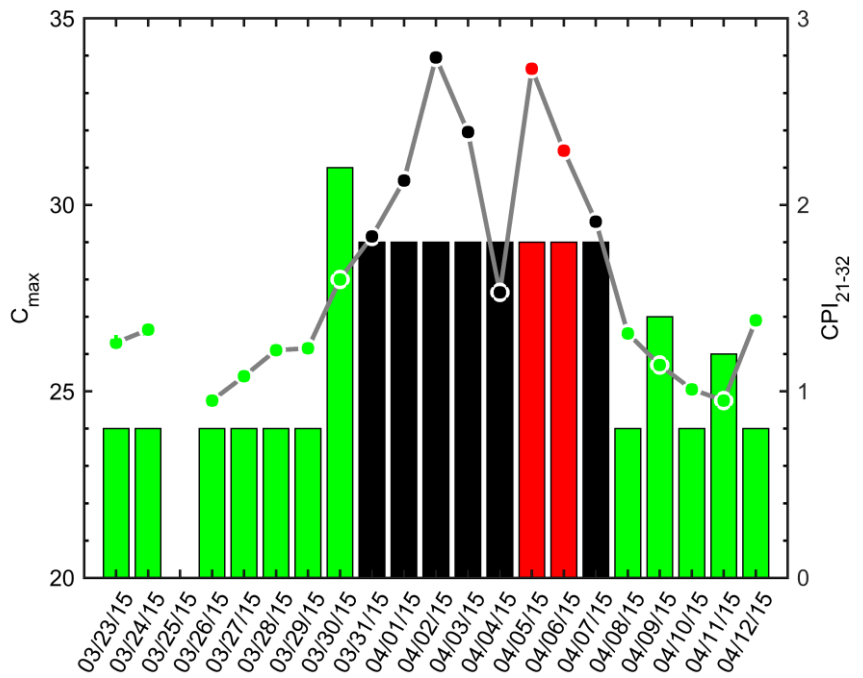


Figure S3. Carbon number of most abundant n-alkane (C_{\max} ; bars) and Carbon Preference Index using n-alkanes from $C_{21}H_{44}$ to $C_{32}H_{66}$ (CPI_{21-32} ; circles).

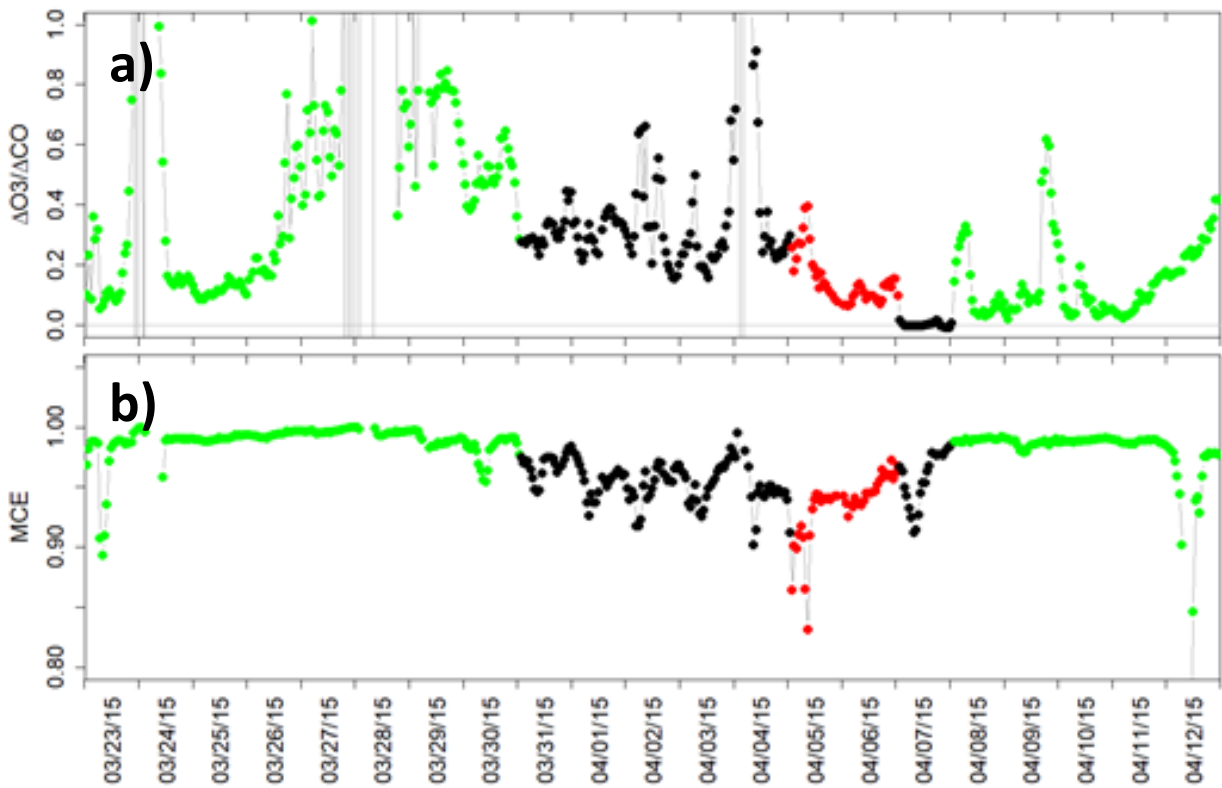


Figure S4. a) Hourly excess ratio between O_3 and CO ($\Delta O_3 / (\Delta CO)$) ranged between 0.00 – 1.00. b) Hourly modified combustion efficiency (MCE: $\Delta CO_2 / (\Delta CO + \Delta CO_2)$) ratios ranged between 0.80 – 1.00 at PDI during the sampling campaign from 23rd March to 12th April 2015. Three colors, including green, black, and red follow the OA clustergram (see main text).

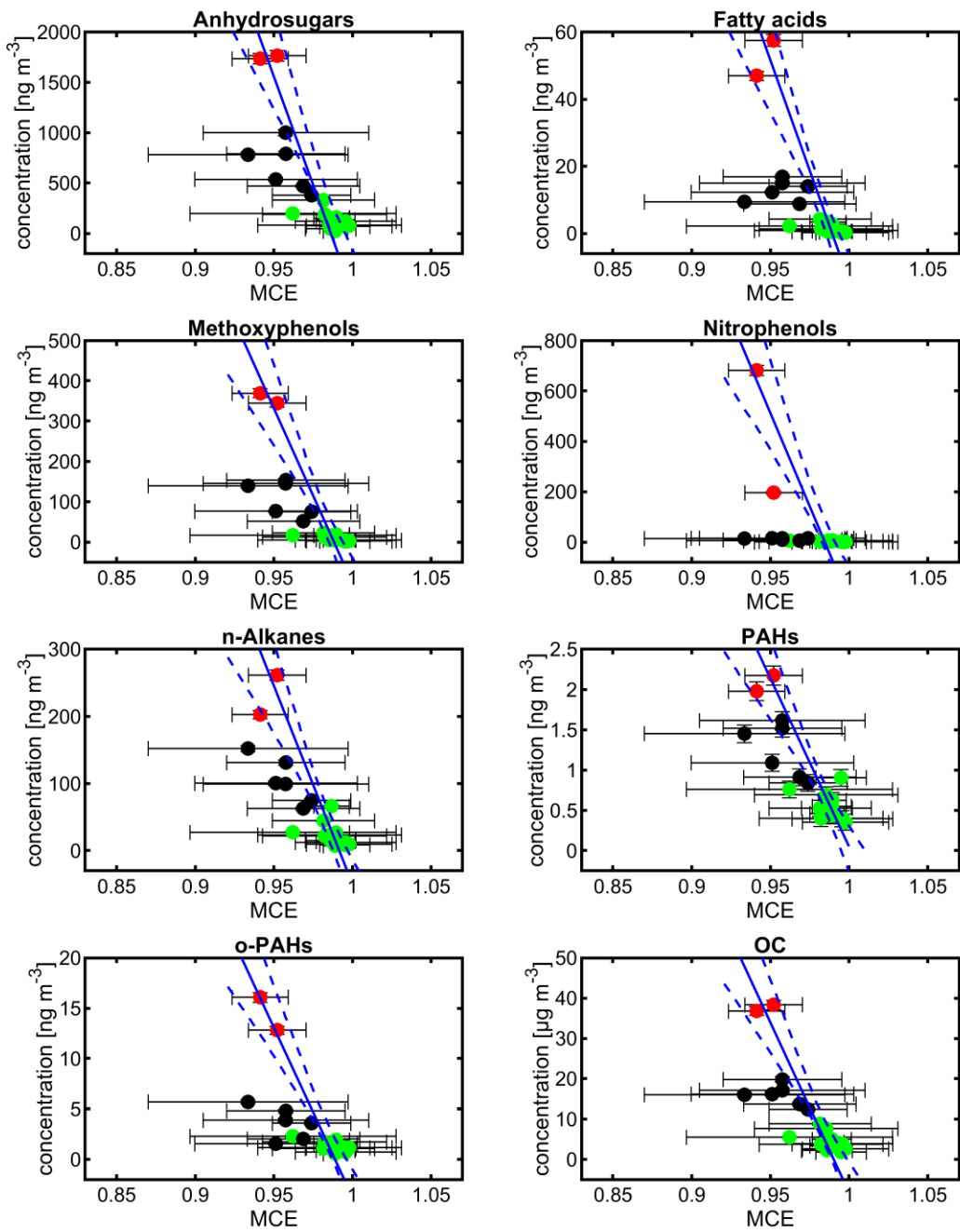


Figure S5. Relation between modified combustion efficiency (MCE) and various compound classes. Dots of green, black and red color correspond to the periods of low-BB, medium and high-BB, respectively. Black errorbars illustrate the uncertainty of each data point (please note that uncertainties for concentrations are too small to be visible in the figure). The blue lines refer to linear fits from Deming regression. Dashed lines denote the non-simultaneous prediction band of the fit function by means of one standard deviation. For most data points, concentration-related errorbars are too small to be visible.

Table S1. Fit coefficients for Deming regression of concentration = $a \cdot MCE + b$ (Figure S4) and their uncertainty by means of one standard deviation from 500 Monte Carlo runs

Compound class	Slope a [ng m^{-3}]	Intercept b [ng m^{-3}]
Anhydrosugars	$-4.30\text{e}4 \pm 1.39\text{e}4$	$4.25\text{e}4 \pm 1.36\text{e}4$
Fatty acids	$-1.31\text{e}3 \pm 420$	$1.30\text{e}3 \pm 410$
Methoxyphenols	$-8.68\text{e}3 \pm 2.70\text{e}3$	$8.58\text{e}3 \pm 2.67\text{e}3$
Nitrophenols	$-1.48\text{e}4 \pm 5.04\text{e}3$	$1.46\text{e}4 \pm 4.89\text{e}3$
n-Alkanes	$-5.90\text{e}3 \pm 5.04\text{e}3$	$5.85\text{e}3 \pm 4.89\text{e}3$
PAHs	-41.8 ± 14.0	41.8 ± 13.7
O-PAHs	-337 ± 101	332 ± 99
OC	$-844\text{e}3 \pm 268\text{e}3$	$836\text{e}3 \pm 263\text{e}3$

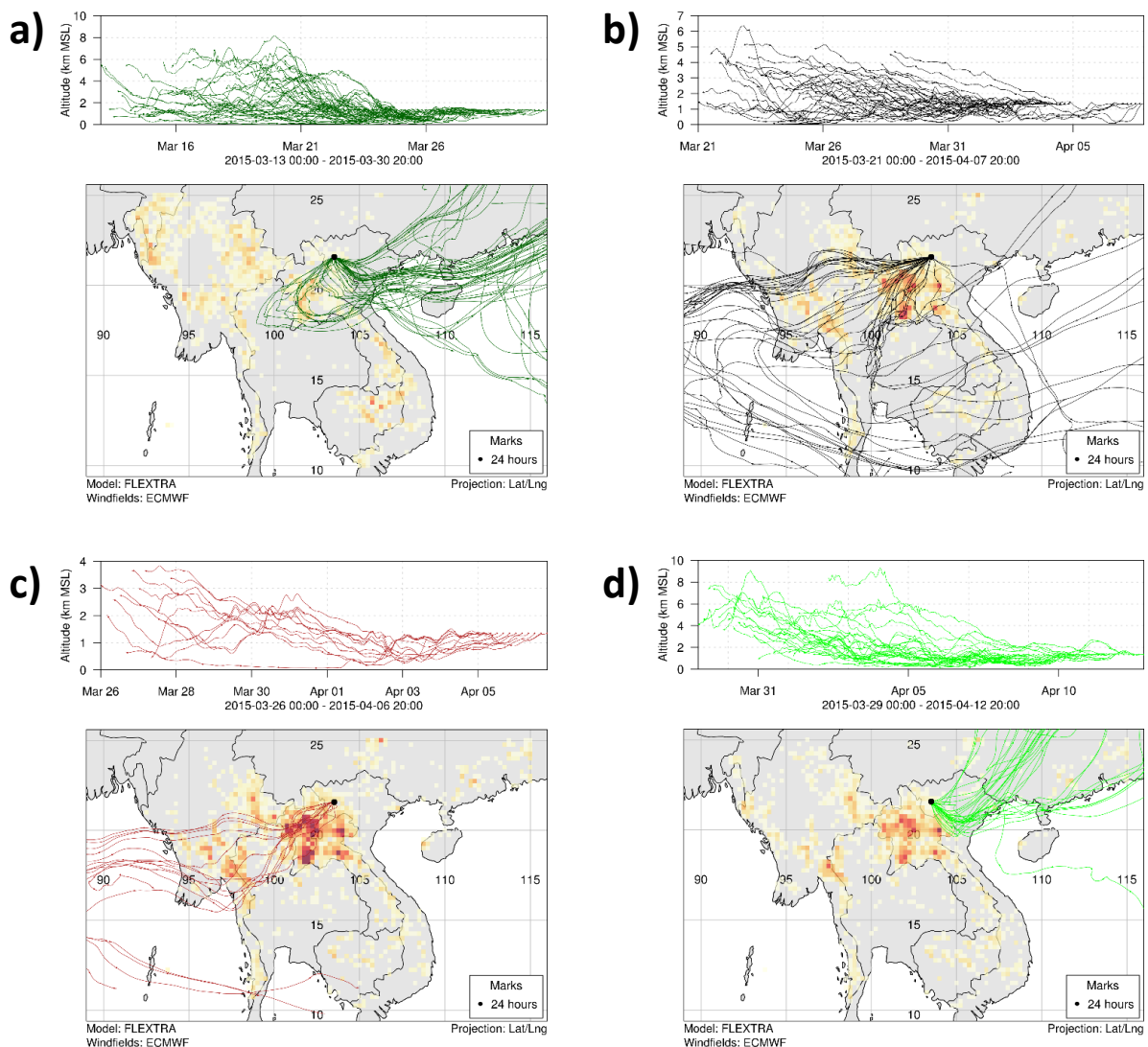


Figure S6. Ten-day backward trajectories arriving at PDI; the sub-periods were determined by the organic aerosol clustering (a) 23 – 30 March ($n=8$), b) 31 March- 4 April + 7 April ($n=6$), c) 05 and 06 April ($n=2$), d) 8 – 12 April ($n=6$). The upper panels display the average height of the trajectories above sea level against time. The lower panel gives the average location of the trajectories overlaid on a map of MODIS fire count densities for the period five days before the beginning of each sub-period until the end of each sub-period (from low (bright yellow) to high (orange-red) fire intensities).